DOI: 10.1002/chem.201002665

Nanocrystal-Based Time–Temperature Indicators

Jie Zeng, Stefan Roberts, and Younan Xia*[a]

Significant progress has been made over the past decade in the chemical synthesis of metal nanocrystals with a wide variety of different shapes.[1] Most of these shapes are not stable in terms of thermodynamic consideration and are expected to spontaneously evolve into new forms with lower surface free energies over different time scales.[2] While this instability poses a tremendous challenge for the preservation of nanocrystals with specific shapes in a solution phase, it also offers a great opportunity to put the nanocrystals to work for some niche applications. Here we present such an example, in which the spontaneous rounding of sharp corners of triangular Ag nanoplates is used to develop a novel class of colorimetric indicators for the time–temperature history or magnitude of acceleration. Such time–temperature indicators can potentially be used for food and medical products, not only as freshness indicators for visualizing the end of a product's shelf-life, but also as environmental tracers for exposing the temperature information during transportation and storage.

We chose triangular Ag nanoplates with relatively sharp corners as a typical example to demonstrate the concept because of the ease of synthesis and their well-established optical properties known as localized surface plasmon resonance (LSPR).[3] Specifically, the Ag nanoplate displays a strong, in-plane dipole resonance mode in the visible region, whose peak position has been found to be highly sensitive to the sharpness of the corners.[4] As the corners of the nanoplate become increasingly rounded, one expects to observe a gradual but significant blue shift for the resonance peak position.

The triangular Ag nanoplates can be synthesized by using a number of methods.[1c,5] In the present work, we prepared the Ag nanoplates by modifying a seed-mediated protocol,[5h] which involves the reduction of $AgNO_3$ by L-ascorbic acid in the presence of Ag seeds, poly(vinyl pyrrolidone) (PVP), and sodium citrate (see Experimental Section for details). Figure S1 a and b in the Supporting Information show transmission electron microscopy (TEM) and high-resolution TEM images of a typical sample. It can be seen that the nanoplate had a triangular cross section along the direction perpendicular to the flat surface, with some slight truncation at the corners. An interesting feature of the Ag nanoplates is that they tend to stack upon each other face-to-face and stand vertically on the TEM grids against one of their edges. From the TEM image, we obtained an average thickness of approximately 5 nm, with edge lengths varying in the range of 30–60 nm. The high-resolution TEM image was recorded from the side face along the [011] direction. The fringe pattern corresponds to a geometrical model, in which the nanoplate is enclosed by two {111} planes as the top and bottom faces and by a mix of {100} and {111} planes as the side faces.[3c,6] The high-resolution TEM image also indicates that there are {111} twin defects and stacking faults parallel to the flat faces of the nanoplate.

In the first demonstration, we placed an aqueous suspension of the triangular nanoplates in a big glass jar, capped it, and then aged it in a water bath at 80 °C for different periods of time. Aliquots (3 mL for each) of the solution were taken from the jar at specific times for taking photographs and UV/Vis extinction spectra. As shown in Figure 1 a, the color of the solution changed notably from cyan to blue, purple, red, and finally yellow over a course of 9 h. Figure 1 b shows the UV/Vis extinction spectra corresponding to the samples depicted in Figure 1 a. The in-plane dipole plasmon peak experienced a blue shift ($\Delta\lambda$) of 320 nm (from 770 nm to 450 nm) during the aging process. Despite the dramatic changes to the in-plane dipole plasmon peak, the out-of-plane, quadruple plasmon resonance peak at 333 nm changed very little, indicating that the platelike morphology was essentially preserved during the thermal aging process.[3c]

Figure 2 shows TEM images of the triangular Ag nanoplates before and after being aged at 80 °C for different periods of time up to 9 h. It is clear that the blue shift observed

[a] Dr. J. Zeng, S. Roberts, Prof. Y. Xia
Department of Biomedical Engineering
Washington University
St. Louis, Missouri 63130 (USA)
E-mail: xia@biomed.wustl.edu

Supporting information for this article is available on the WWW under http://dx.doi.org/10.1002/chem.201002665.

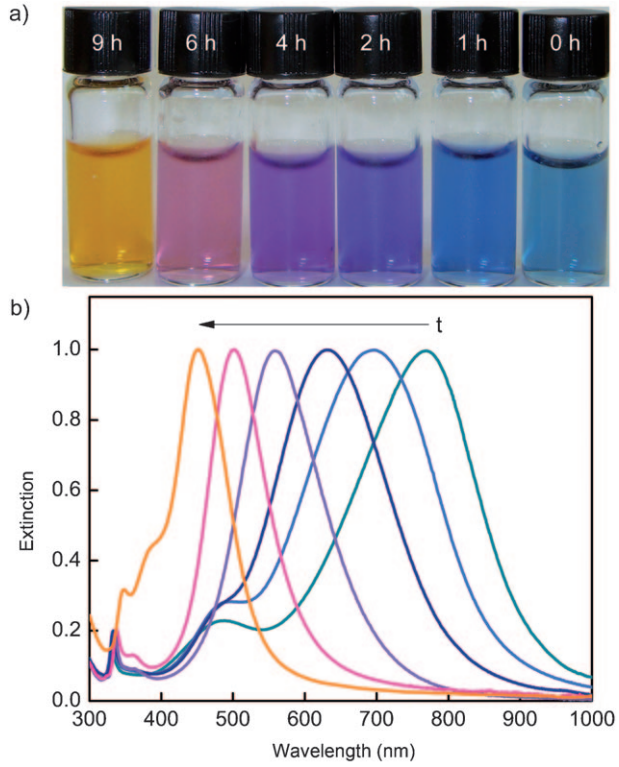

Figure 1. a) Photograph of the samples after they had been subjected to aging at 80 °C in air for different periods of time. b) UV/Vis extinction spectra taken from the corresponding samples shown in a).

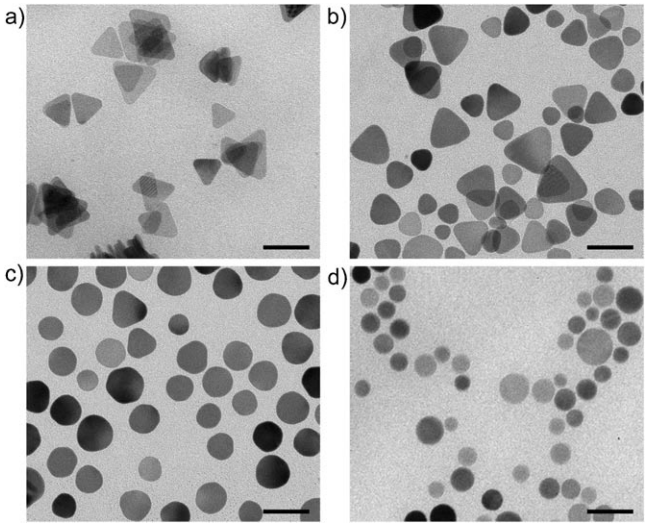

Figure 2. TEM images of the triangular Ag nanoplates after they had been aged at 80 °C for a) 0 h, b) 1 h, c) 4 h, and d) 9 h, respectively. The sharp corners of the Ag nanoplates were gradually rounded to generate circular disks with reduced lateral dimensions. Scale bars, 50 nm.

for the in-plane dipole plasmon resonance peak is a manifestation of the morphological changes occurred to the Ag nanoplates. Specifically, during the aging process, the sharp corners of the Ag nanoplates gradually became rounded, eventually leading to the formation of circular disks. The histogram shown in Figure S2 summarizes the results of our statistical analysis of the size distributions of triangular nanoplates and circular disks. Two distinct populations of particle sizes are found for the initial, triangular nanoplates. In addition, these populations remained essentially the same throughout the aging process. Compared to the original triangular plates, the circular disks had an obvious reduction in lateral dimensions and an increase in thickness from approximately 5 nm to 8–9 nm (as revealed by the plates with a vertical orientation shown in Figure S1 c in the Supporting Information). These results are consistent with previous observations briefly reported in the literature.[7]

To fully demonstrate the potential of these Ag nanoplates as time–temperature indicators (TTIs), we also conducted the aging process at three other temperatures: 4 °C, 25 °C, and 47 °C. As shown in Figure 3 a, the aqueous suspensions of Ag nanoplates exhibited a similar blue shift as a function of time. Evidently, the rate of shift (nm per day) had a strong correlation with the temperature: it was dramatically slowed down as the temperature for aging was reduced. The different rates of response to temperature should be particularly useful for accurate and sensitive recording of the time–temperature history of a product. Aside from indicating the shelf-life of a product, the nanocrystal-based TTIs can also

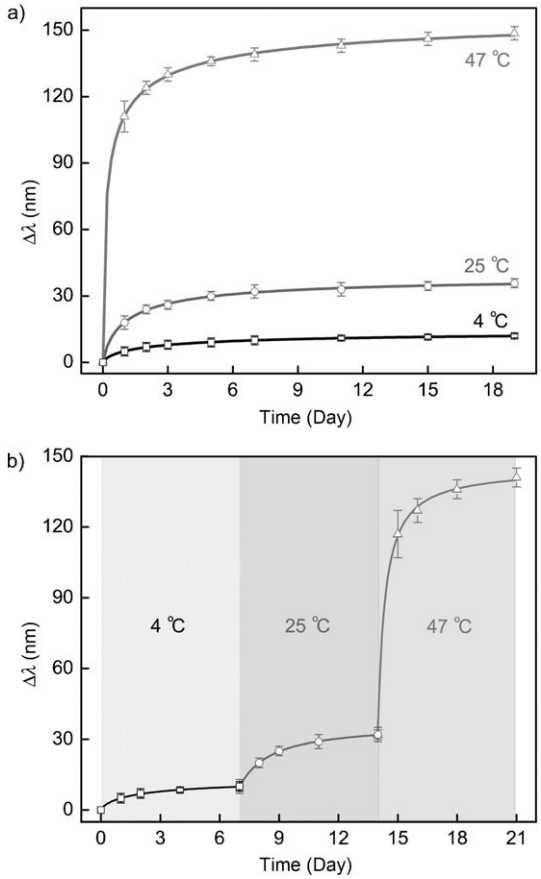

Figure 3. a) Plots of the peak shift as a function of time when the same batch of triangular Ag nanoplates as in Figure 1 was aged at 4 °C, 25 °C, and 47 °C, respectively. b) A plot showing the cumulative effect of a combination of three different time–temperature exposures.

be used to expose the distribution chain of a given product, including transportation and storage. Figure 3b shows a plot of the cumulative effect from a combination of three different time–temperature exposures.

Interestingly, the Ag nanoplate-based indicators are also sensitive to both the magnitude and duration of acceleration. In a typical experiment, we subjected an aqueous suspension of the triangular Ag nanoplates to eight rounds of centrifugation at 22000 *g* (in relative centrifugal force or RCF) with each round lasting 20 min. We then took an aliquot from the supernatant after each round of centrifugation for UV/Vis spectroscopy measurement. The in-plane dipole plasmon peak experienced a continuous blue shift with respect to the rounds of centrifugation. We observed a total blue shift of approximately 230 nm (see Figure S3 in the Supporting Information) after eight rounds. The solution showed color changes after each round of centrifugation, albeit the change was more dramatic after five rounds.

To demonstrate the effect of acceleration magnitude on the nanoplates, we conducted two additional sets of experiments at 14000 *g* and 7000 *g* in RCF. As shown in Figure 4a, the spectral shift became less significant as the magnitude of acceleration was reduced. Note that the dependence for each set of data (22000 *g*, 14000 *g*, or 7000 *g*) was not linear as the round of centrifugation was increased. Rather, the peak shifted slowly during the first couple of rounds and then increased quickly until reaching a plateau. Figure 4b shows the dependence of peak shift as a function of the magnitude of acceleration, where the samples were subjected to five rounds of centrifugation before recording the spectrum. It is clear that the peak was blue-shifted more significantly as the magnitude of centrifugation was increased. TEM images taken from the samples that had been subjected to centrifugation at 22000 *g* in RCF show once again a good correlation between the blue shift and rounding of corners for the triangular Ag nanoplates (see Figure S4 in the Supporting Information). The only difference between thermal aging and centrifugation is that some of some of the Ag nanoplates attached to each other and fused together in the case of centrifugation.

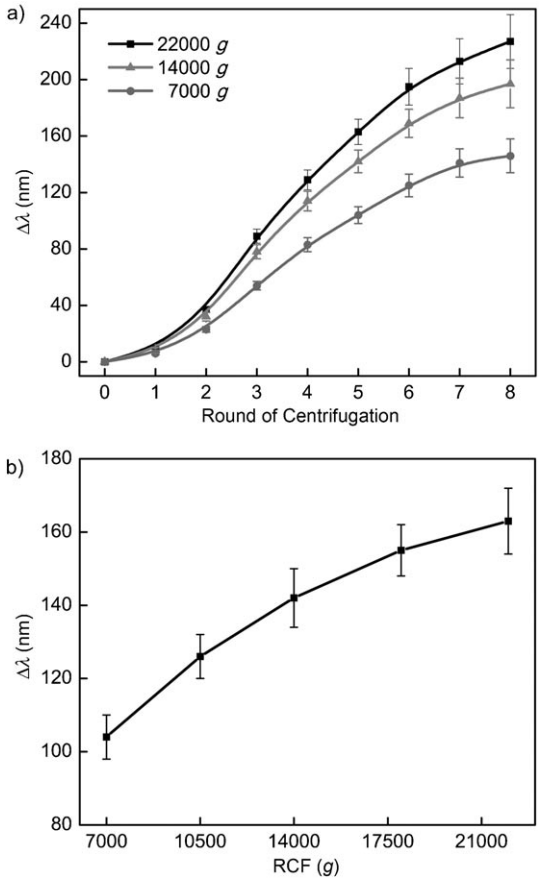

Figure 4. a) Plots of the peak shift as a function of the round of centrifugation at 22000 *g*, 14000 *g*, and 7000 *g* in RCF. For each round of centrifugation, the process lasted 20 min. b) Plots of the peak shift as a function of RCF. For each RCF, the samples were centrifuged for five rounds with each round lasting 20 min.

The corners of the Ag nanoplates could be rounded through two different mechanisms: oxidative etching and atomic migration across the surface. During the process of either aging or centrifugation, oxygen in the medium can preferentially oxidize the atoms at highly energetic sites (such as the corners) through reaction (1):

$$4Ag^0 + O_2 + 2H_2O \rightarrow 4Ag^+ + 4OH^- \quad (1)$$

The resultant Ag^+ ions could be reduced and deposited at less energetic sites of the nanoplate due to the existence of some residual reductant such as L-ascorbic acid and PVP in the solution. To examine the role played by oxygen in the aging process, we monitored the spectral shift as a function of time for triangular Ag nanoplates (from the same batch as those used for Figure 1) that were bubbled with Ar at 4°C, 25°C, and 47°C, respectively (see Figure S5 in the Supporting Information). Compared to the experiments conducted under ambient conditions, the extents of peak shift were only slightly reduced when the samples were bubbled and protected with Ar. This observation indicates that oxidative etching did not play a significant role in rounding the corners of Ag nanoplates. Alternatively, the corners were rounded through direct migration of Ag atoms across the surface. Furthermore, the fact that the populations of particle sizes remained the same throughout the aging process (see Figure S2 in the Supporting Information) is also consistent with the migration mechanism we proposed here. In this case, direct migration of atoms across the surface of individual particles would not affect the size populations. In practice, this mechanism will allow us to use the present TTIs as sealed samples. It should be pointed out that for each temperature under Ar protection, the peak shift tended to reach a plateau after a few days, while it would keep increasing with time for the case in air. This observation suggests that oxidative etching is a much slower process that could be stretched over a longer period of time than

atomic migration across the surface. As for centrifugation, it can accelerate the migration of Ag atoms across the surface of Ag nanoplates due to the increased shear force, resulting in a faster shift for the peaks as compared to thermal aging.

To confirm the surface migration mechanism, we deposited triangular Ag nanoplates on a substrate such as a TEM grid to prevent the Ag species from moving freely as they did in an aqueous solution. As shown in Figure S6 in the Supporting Information, after storage in air for two months, each triangular Ag nanoplate was transformed into irregularly shaped nanoparticles scattered around the initial site of the plate. In contrast, when we subjected circular Ag nanodisks to the same condition, no significant change to the shape was observed within a period of two months. These observations suggest that the migration of atoms across the surface, which is highly dependent on the shape of a nanostructure, is an intrinsic property of Ag that does not depend on the solvent or environment. Instead, it highly depends on the shape or morphology of a nanocrystal as surface free energy has a strong correlation with the curvature.

We also estimated the energy involved in the morphological change from a triangular plate to a circular disk. Assuming the total volume is conserved during the transformation, we can use a simple, ideal model to describe this process (see Figure S7 in the Supporting Information), in which the effect of solvent or substrate was not considered. The change in surface energy (ΔE_s) can be presented as given in Equation (2),

$$\Delta E = \gamma\left(\frac{\sqrt{3}}{2}a^2 + 3ad_1 - 2\pi r^2 - 2\pi r d_2\right) \quad (2)$$

where γ is the surface tension of silver [$0.72\ \mathrm{N\,m^{-1}}$];[8] a and d_1 are the side length and thickness of the triangular plates; and r and d_2 are the radius and thickness of the circular disks. This change in surface energy can be broken down into three major components: kinetic energy (E_k), heat (E_h) generated by friction during the migration of Ag atoms, and increased internal energy (ΔE_i, that is, sum of anti-stacking fault energies) that is located at the newly formed stacking faults in a circular disk. According to the expressions (see the Supporting Information for details), these energies can be estimated as: E_k ($\approx 10^{-39}$ J) $< E_h$ ($\approx 10^{-30}$ J) $< \Delta E_i$ ($\approx 10^{-16}$ J) $\approx$ ΔE_s ($\approx 10^{-16}$ J). It can be concluded that the corner rounding of Ag nanoplates is always accompanied by an energy transfer from surface energy to internal energy.

In summary, we have demonstrated that the intrinsic instability of nanocrystals can be used to realize a novel application. As shown in this work, the "instable" Ag nanoplates can serve as indicators of time and temperature for various commercial needs. At the moment, it is still difficult to resolve the reaction orders and activation energies involved in the shape transformation of triangular Ag nanoplates. However, the intrinsic structural instability and striking color changes associated with triangular Ag nanoplates make them particularly useful as a reliable recorder of environmental factors. As compared to other existing commercial monitoring systems, the nanocrystal-based indicators might provide a number of merits, including lower cost, easier to produce, and simpler for detection either by naked eye or a UV/Vis spectrometer.

Experimental Section

Preparation of Ag seeds: In a typical synthesis of Ag seeds, 11 mL of an aqueous solution containing 0.11 mM silver nitrate ($AgNO_3$, Aldrich) and 2.05 mM trisodium citrate (Aldrich) was prepared. Under magnetic stirring, an aqueous solution of sodium borohydride ($NaBH_4$, Fisher) (0.3 mL, 5 mM) was added all at once. Stirring was stopped after 10 min. The seeds were used after aging for 5 h.

Preparation of triangular Ag nanoplates: The Ag nanoplates were prepared using a seed-mediated procedure with a few modifications.[5h] In a typical synthesis, 100 mL of ultrapure water was mixed with aqueous $AgNO_3$ (2.5 mL, 5 mM), aqueous poly(vinyl pyrrolidone) (PVP, MW $\approx$29,000, Aldrich) (7.5 mL, 0.7 mM), aqueous sodium citrate (7.5 mL, 30 mM), and 0.2 mL of the seed solution, followed by slow dropping into aqueous L-ascorbic acid (Aldrich) (62.5 mL, 1 mM). Under magnetic stirring, the color of the solution changed gradually during the dropping of L-ascorbic acid and was finally stable at cyan. The product was directly used for time-temperature tests without further purification or treatment.

Time–temperature tests: An aqueous suspension of the triangular Ag nanoplates was placed in a big glass jar (VWR, CAT. NO. 89000–234, 100 mL), capped, and then aged in a water bath at 4, 25, 47, or 80 °C for different periods of time. Aliquots of the solution were taken out from the jar at specific time for photographs and UV/Vis extinction spectral recordings.

Acceleration tests: 1.5 mL centrifugation tubes containing 1.0 mL of aqueous suspensions of the triangular Ag nanoplates were subjected to centrifugation for eight rounds at 7000 *g*, 10500 *g*, 14000 *g*, 18000 *g*, or 22000 *g* in RCF with each round lasting 20 min. The centrifugation was performed in a thermostatic chamber with a constant temperature at 4 °C. After the completion of each round of centrifugation, 0.6 mL of the supernatant was removed from the tubes and replaced with 0.6 mL of ultrapure water. The nanoplates were re-suspended in an aqueous solution. A photograph was taken for samples after centrifugation for different rounds (Figure S3a, at 22000 *g* in RCF), and a UV/Vis extinction spectrum was taken for each sample to determine $\Delta\lambda$ (see Figure S3b in the Supporting Information).

Characterization of Ag nanoplates by TEM and UV/Vis spectroscopy: TEM images were captured by using a Phillips 420 microscope operated at 120 kV. High-resolution TEM images were taken on a JEOL 3000F high-resolution transmission electron microscope operated at 300 kV. The samples for TEM studies were prepared by drying a drop of the aqueous suspension of particles on a piece of carbon-coated copper grid (Ted Pella, Redding, CA) under ambient conditions. The sample was dried and stored in a vacuum for TEM characterization. The UV/Vis extinction spectra were obtained using a Varian Cary 50 UV/Vis spectrophotometer.

Acknowledgements

This work was supported in part by a research grant from the NSF (DMR-0804088) and startup funds from Washington University in St. Louis. Y.X. was also partially supported by the World Class University (WCU) program through the National Research Foundation of Korea funded by the Ministry of Education, Science and Technology (R32-20031). Part of the research was performed at the Nano Research Facility (NRF), a member of the National Nanotechnology Infrastructure Network (NNIN), which is supported by the NSF under award no. ECS-

0335765. We thank J. Tao and Y. M. Zhu at Brookhaven National Laboratory for technical assistance with the high-resolution TEM measurements.

Keywords: nanoparticles · sensors · silver · time–temperature indicators

[1] a) T. S. Ahmadi, Z. L. Wang, T. C. Green, A. Henglein, M. A. El-Sayed, *Science* **1996**, *272*, 1924; b) R. D. Averitt, D. Sarkar, N. J. Halas, *Phys. Rev. Lett.* **1997**, *78*, 4217; c) R. Jin, Y. W. Cao, C. A. Mirkin, K. L. Kelly, G. C. Schatz, J. G. Zheng, *Science* **2001**, *294*, 1901; d) V. F. Puntes, K. M. Krishnan, A. P. Alivisatos, *Science* **2001**, *291*, 2115; e) N. R. Jana, L. Gearheart, C. J. Murphy, *J. Phys. Chem. B* **2001**, *105*, 4065; f) Y. G. Sun, Y. N. Xia, *Science* **2002**, *298*, 2176; g) N. Tian, Z. Y. Zhou, S. G. Sun, Y. Ding, Z. L. Wang, *Science* **2007**, *316*, 732; h) A. R. Tao, S. Habas, P. D. Yang, *Small* **2008**, *4*, 310.

[2] a) A. P. Alivisatos, *Science* **1996**, *271*, 933; b) C. Burda, X. B. Chen, R. Narayanan, M. A. El-Sayed, *Chem. Rev.* **2005**, *105*, 1025.

[3] a) K. L. Kelly, E. Coronado, L. L. Zhao, G. C. Schatz, *J. Phys. Chem. B* **2003**, *107*, 668; b) K. A. Willets, R. P. Van Duyne, *Annu. Rev. Phys. Chem.* **2007**, *58*, 267; c) J. E. Millstone, S. J. Hurst, G. S. Métraux, J. I. Cutler, C. A. Mirkin, *Small* **2009**, *5*, 646; d) I. Pastoriza-Santos, L. M. Liz-Marzán, *J. Mater. Chem.* **2008**, *18*, 1724.

[4] J. Nelayah, M. Kociak, O. Stéphan, F. J. G. De Abajo, M. Tencé, L. Henrard, D. Taverna, I. Pastoriza-Santos, L. M. Liz-Marzán, C. Colliex, *Nat. Phys.* **2007**, *3*, 348.

[5] a) I. Pastoriza-Santos, L. M. Liz-Marzán, *Nano Lett.* **2002**, *2*, 903; b) S. H. Chen, D. L. Carroll, *Nano Lett.* **2002**, *2*, 1003; c) R. Jin, Y. C. Cao, E. Hao, G. S. Métraux, G. C. Schatz, C. A. Mirkin, *Nature* **2003**, *425*, 487; d) Y. G. Sun, Y. N. Xia, *Adv. Mater.* **2003**, *15*, 695; e) Y. G. Sun, B. Mayers, Y. N. Xia, *Nano Lett.* **2003**, *3*, 675; f) G. S. Métraux, C. A. Mirkin, *Adv. Mater.* **2005**, *17*, 412; g) I. Washio, Y. J. Xiong, Y. D. Yin, Y. N. Xia, *Adv. Mater.* **2006**, *18*, 1745; h) D. Aherne, D. M. Ledwith, M. Gara, J. M. Kelly, *Adv. Funct. Mater.* **2008**, *18*, 2005.

[6] Z. L. Wang, *J. Phys. Chem. B* **2000**, *104*, 1153.

[7] Q. Zhang, J. Ge, T. Pham, J. Goebl, Y. Hu, Z. Lu, Y. Yin, *Angew. Chem.* **2009**, *121*, 3568; *Angew. Chem. Int. Ed.* **2009**, *48*, 3516.

[8] S. F. Chernov, Y. V. Fedorov, V. N. Zakharov, *J. Phys. Chem. Solids* **1993**, *54*, 963.

Received: September 16, 2010
Published online: October 13, 2010

